ASTROBIOLOGY
Volume 20, Number 5, 2020

DOI: 10.1089/ast.2019.2060

Large Mass-Independent Oxygen Isotope Fractionations in Mid-Proterozoic Sediments: Evidence for a Low-Oxygen Atmosphere?

Noah J. Planavsky,[1] Christopher T. Reinhard,[2] Terry T. Isson,[3] Kazumi Ozaki,[4] and Peter W. Crockford[5,6]

Abstract

Earth's ocean-atmosphere system has undergone a dramatic but protracted increase in oxygen (O_2) abundance. This environmental transition ultimately paved the way for the rise of multicellular life and provides a blueprint for how a biosphere can transform a planetary surface. However, estimates of atmospheric oxygen levels for large intervals of Earth's history still vary by orders of magnitude—foremost for Earth's middle history. Historically, estimates of mid-Proterozoic (1.9–0.8 Ga) atmospheric oxygen levels are inferred based on the kinetics of reactions occurring in soils or in the oceans, rather than being directly tracked by atmospheric signatures. Rare oxygen isotope systematics—based on quantifying the rare oxygen isotope ^{17}O in addition to the conventionally determined ^{16}O and ^{18}O—provide a means to track atmospheric isotopic signatures and thus potentially provide more direct estimates of atmospheric oxygen levels through time. Oxygen isotope signatures that deviate strongly from the expected mass-dependent relationship between ^{16}O, ^{17}O, and ^{18}O develop during ozone formation, and these ''mass-independent'' signals can be transferred to the rock record during oxidation reactions in surface environments that involve atmospheric O_2. The magnitude of these signals is dependent upon pO_2, pCO_2, and the overall extent of biospheric productivity. Here, we use a stochastic approach to invert the mid-Proterozoic $\Delta^{17}O$ record for a new estimate of atmospheric pO_2, leveraging explicit coupling of pO_2 and biospheric productivity in a biogeochemical Earth system model to refine the range of atmospheric pO_2 values that is consistent with a given observed $\Delta^{17}O$. Using this approach, we find new evidence that atmospheric oxygen levels were less than $\sim$1% of the present atmospheric level (PAL) for at least some intervals of the Proterozoic Eon. Key Words: Proterozoic—Atmospheric oxygenation—Precambrian—Triple oxygen. Astrobiology 20, 628–636.

1. Introduction

The mid-Proterozoic (1.9 to 0.8 billion years ago, Ga) is generally regarded as a transitional time between the anoxic surface conditions of the Archean and the relatively well-oxygenated conditions that characterized much of the late Neoproterozoic and Phanerozoic (Canfield, 1998, 2005; Holland, 2006; Kump, 2008; Derry, 2015; Laakso and Schrag, 2017). However, there exists a wide range of estimates for surface oxygen during the mid-Proterozoic, from <0.1% to 40% of the present atmospheric level (PAL) (Kump, 2008; Lyons *et al.,* 2014). If estimates of mid-Proterozoic pO_2 levels near or below $\sim$1% (PAL) are correct, environmental conditions characteristic of the majority of Earth's history may have limited ecosystem complexity and could have impacted the emergence and ecological expansion of mobile multicellular heterotrophs (Reinhard *et al.,* 2016). The potential for low pO_2 levels during the mid-Proterozoic also has important implications for oxygen-based frameworks for remote life detection on terrestrial planets. In particular, if we use Earth as an analogue and take lower Proterozoic pO_2 estimates, it is possible that terrestrial planets can stabilize for billion-year timescales at weakly oxygenated states, with implications for atmospheric biosignature detection (Reinhard *et al.,* 2017). The importance of the mid-Proterozoic for the secular history of Earth's biotic

[1]Department of Geology and Geophysics, Yale University, New Haven, Connecticut, USA.
[2]School of Earth and Atmospheric Sciences, Georgia Institute of Technology, Atlanta, Georgia, USA.
[3]Environmental Research Institute, University of Waikato, Tauranga, New Zealand.
[4]Department of Environmental Science, Toho University, Funabashi, Chiba, Japan.
[5]Department of Earth and Planetary Sciences, Weizmann Institute of Science, Rehovot, Israel.
[6]Department of Geosciences, Princeton University, Princeton, New Jersey, USA.

and environmental evolution thus provides strong motivation to critically assess claims of low surface oxygen levels through this interval.

Historically, mid-Proterozoic atmospheric oxygen levels were assumed to be ~10% PAL based on geochemical signatures in paleosols and marine redox records (Holland, 2006; Kump, 2008). There are several reports of Proterozoic paleosols with quantitative iron oxidation, implying atmospheric oxygen levels above ~1% PAL (Pinto and Holland, 1988; Zbinden *et al.,* 1988). The presence of anoxic deep oceans (*e.g.,* Poulton *et al.,* 2010; Lyons *et al.,* 2014) has been assumed to roughly constrain maximum atmospheric oxygen levels at ~40% (Canfield, 1998; Kump, 2008). However, these traditional bounding pO_2 estimates have recently been questioned (Planavsky *et al.,* 2018). Critically, the only definitive mid-Proterozoic paleosols that have formed directly from parent rock are characterized by iron loss (Mitchell and Sheldon, 2009, 2010, 2016), pointing to low oxygen levels. A suite of other proxies has also suggested atmospheric oxygen levels less than ~10% PAL or even ~1% PAL, for at least intervals of the mid-Proterozoic. For instance, sedimentary Cr isotopes and carbonate trace element patterns have been suggested to indicate atmospheric oxygen levels less than 1% PAL, perhaps as low as 0.1% PAL (Cole *et al.,* 2016; Gilleaudeau *et al.,* 2016; Liu *et al.,* 2016; Bellefroid *et al.,* 2018), consistent with updated currently available mid-Proterozoic paleosol records. However, records of both low and high mid-Proterozoic oxygen levels (Zhang *et al.,* 2016b) have been questioned and critiqued (Planavsky *et al.,* 2016).

Some of the debate surrounding Proterozoic oxygen levels emerges naturally from the diverse suite of proxies being applied to the problem. The majority of paleo-oxygen barometers do not directly track an atmospheric signal; instead, they track an oxidation reaction occurring in a soil (or the oceans), or they attempt to link a marine redox structure to an atmospheric oxygen level. These approaches, even those that rely on fossilized soil horizons in more direct contact with the overlying atmosphere, can only indirectly track pO_2 and rely on a large number of assumptions. For instance, to link a paleosol record to an atmospheric oxygen level one must assume a background pCO_2, local rainfall and infiltration rates, and a denudation rate, in addition to assumptions regarding the presence/absence and/or activity of a local terrestrial biosphere. To link a marine redox-sensitive metal signature to an atmospheric pO_2 estimate one needs to link local or global ocean redox to atmospheric composition and is thus reliant on a series of assumptions regarding ocean circulation and nutrient inventories. Not surprisingly, different researchers have reached very different conclusions about Proterozoic oxygen levels using essentially the same numerical frameworks and empirical records. The strong potential for diagenetic overprinting of depositional signatures in paleoredox proxies only adds to uncertainty and continuing debate.

The sedimentary triple-oxygen isotope record presents a means to more directly track mid-Proterozoic atmospheric oxygen levels. The majority of reactions on Earth induce stable isotope fractionations that are dictated almost entirely by mass differences between isotopes (Urey, 1947). However, for systems with more than two isotopes, certain processes can create pools that are anomalously enriched or depleted in a given isotope relative to what would be expected for a purely mass-dependent process, leading to so called ''mass-independent'' or ''non-mass-dependent'' (NMD) isotope effects (*e.g.,* Thiemens, 2006). Ozone formation is one of the most intensively studied of the these NMD isotope effects (Thiemens and Heidenreich, 1983). Ozone formed in the stratosphere is anomalously enriched in ^{17}O, denoted as a positive $\Delta^{17}O$ value. This positive $\Delta^{17}O$ signal is transferred via photochemistry to atmospheric CO_2, while the complementary negative $\Delta^{17}O$ signal is stored in residual stratospheric O_2. The magnitude of the negative $\Delta^{17}O$ anomaly in atmospheric oxygen is dependent most strongly on the amount of atmospheric O_2 and CO_2 and how quickly the anomalous O_2 produced during photochemistry is reset by biological cycling (Luz *et al.,* 1999; Cao and Bao, 2013). This residual negative $\Delta^{17}O$ signal can then be transferred to the rock record via oxidation reactions during weathering (*e.g.,* pyrite oxidation). Therefore, the $\Delta^{17}O$ composition of sedimentary sulfate minerals at any given time and location primarily reflects (1) atmospheric O_2 levels; (2) atmospheric CO_2 levels; and (3) biospheric O_2 recycling (*e.g.,* primary productivity) (Luz *et al.,* 1999; Cao and Bao, 2013). Importantly, once atmospheric oxygen isotope signatures are imparted to sulfate diagenetic processes, microbial sulfur cycling and/or metamorphic overprinting should only act to erase $\Delta^{17}O$ anomalies, making this proxy in many cases more robust than traditional redox proxies.

Here, we revisit previous modeling of the Proterozoic sulfate mineral $\Delta^{17}O$ record (Crockford *et al.,* 2018a, 2019; Hodgskiss *et al.,* 2019) in order to more precisely reconstruct atmospheric pO_2 during an interval of mid-Proterozoic time. We utilize a stochastic approach, building from statistical analysis of output from the global biogeochemical model CANOPS (Ozaki *et al.,* 2011, 2019), to filter the large number of mathematically possible solutions for any given $\Delta^{17}O$ value according to only those solutions that allow for mass balance between biospheric productivity and atmospheric pO_2. This results in a dramatically reduced number of possible O_2-CO_2-productivity combinations consistent with a given $\Delta^{17}O$ measurement, and a much more precise range of atmospheric pO_2 values.

2. The Mid-Proterozoic $\Delta^{17}O$ Record

Sulfate minerals extracted thus far from mid-Proterozoic carbonates have been found to be heavily contaminated with recent atmospheric sulfate and thus cannot be used to track atmospheric signals (Peng *et al.,* 2014). However, sulfate from a limited number of mid-Proterozoic evaporite successions appears to preserve $\Delta^{17}O$ signals from atmospheric O_2, presumably acquired during terrestrial pyrite oxidation (Crockford *et al.,* 2018a). Although $\Delta^{17}O$ signals in examined evaporite successions are highly variable, there are distinctively negative $\Delta^{17}O$ signals relative to the Phanerozoic sulfate record (Crockford *et al.,* 2018a) (Fig. 1). These signals are thought to capture negative $\Delta^{17}O$ anomalies from tropospheric O_2. Here we assume that between 5% and 15% of the oxygen atoms that become incorporated into sulfate during pyrite oxidation are atmospherically derived (Balci *et al.,* 2007; see discussion in Crockford *et al.,* 2018a; Kohl and Bao, 2011). This range is slightly lower than a recent estimate of ~18% atmospheric oxygen in sulfate from the

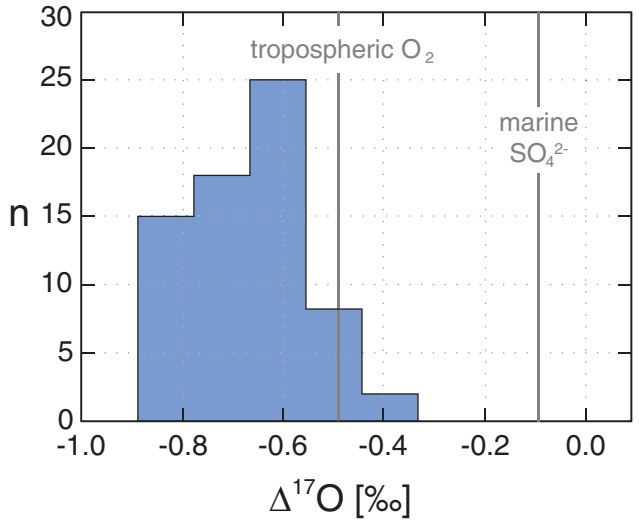

FIG. 1. Histogram of gypsum $\Delta^{17}O$ values from the *ca.* 1.4 Ga lacustrine Sibley Basin in Ontario, Canada. This lacustrine setting seems to be characterized by limited sulfur cycling (sulfur reduction and re-oxidation; see Crockford *et al.,* 2018a), allowing for the effective preservation of atmospheric $\Delta^{17}O$ anomalies. For comparison, the gray lines show the compiled values of modern marine sulfate and modern tropospheric O_2. Note that only a portion (roughly 10%) of atmospheric oxygen is incorporated into sulfate during pyrite oxidation. Data adapted from Crockford *et al.* (2018a) and Hodgskiss *et al.* (2019). Color images are available online.

strongly anthropogenically influenced Mississippi River system (Killingsworth *et al.,* 2018).

Variability on the formation scale in existing mid-Proterozoic evaporite $\Delta^{17}O$ data sets is expected, given that any surface sulfur cycling will tend to homogenize and erase $\Delta^{17}O$ signals. In particular, activation of S to SO_3^{2-} during microbial sulfate reduction leads to extremely rapid O isotope equilibration with isotopically ''normal'' ambient H_2O within the cell (*e.g.,* Antler *et al.,* 2013). Therefore, sulfate reduction and sulfide oxidation will tend to decrease the magnitude of $\Delta^{17}O$ signals. Marine environments, even those that are strongly redox stratified (*e.g.,* the Black Sea), are characterized by extensive sulfide re-oxidation (Yakushev and Neretin, 1997). Evaporative successions can similarly be marked by high rates of sulfur redox cycling (*e.g.,* Petrash *et al.,* 2012). With these observations in mind, it is not surprising that there is variation within a given evaporite unit and that the most anomalous $\Delta^{17}O$ signals have thus far been found in lacustrine—rather than marine—evaporite successions (Crockford *et al.,* 2018a). The most negative $\Delta^{17}O$ signals found to date with the exception of Cryogenian barite and CAS (*cf.* Bao *et al.,* 2008; Crockford *et al.,* 2016)—$\Delta^{17}O$ values of -0.9‰ (Fig. 1)—are observed in the lacustrine Sibley Formation in Canada, deposited at ~1.4 Ga (Crockford *et al.,* 2018a). However, similarly anomalously negative values ($\Delta^{17}O < -0.75$‰) are also found in the *ca.* 1.7 Ga marine Myrtle Shale in the MacArthur Basin in Australia (Crockford *et al.,* 2019) and the *ca.* 1.9 Ga marine Belcher Group in Canada (Hodgskiss *et al.,* 2019). Therefore, although the mid-Proterozoic sedimentary $\Delta^{17}O$ record is still sparse, motivating additional work, there is a clear signal from several formations for markedly different sulfate $\Delta^{17}O$ values than those observed from the modern and recent Earth system. Because minimum values are likely our best estimate of a true atmospheric signal (Crockford *et al.,* 2018a; Planavsky *et al.,* 2018), in what follows we develop an approach that is designed to translate these anomalously low values into a quantitative estimate of atmospheric pO_2. However, we stress that current records are unlikely to capture ''true'' minimum sulfate $\Delta^{17}O$ values, indicating that our approach should be viewed as providing maximum pO_2 estimates.

3. Translating $\Delta^{17}O$ Signals to pO_2 Estimates

The first step in our approach uses a 4-box atmosphere-ocean-biosphere model derived from that of Cao and Bao (2013) (Fig. 2) to estimate all combinations of atmospheric pO_2 and biospheric O_2 recycling that are consistent with a given $\Delta^{17}O$ value. The model is designed to predict tropospheric $\Delta^{17}O$ solutions with different pO_2, pCO_2, and O_2 residence times (*e.g.,* biospheric O_2 recycling rates). $\Delta^{17}O$ values of stratospheric O_2 and CO_2 vary with changing pO_2/pCO_2 ratios, following experimental results from the O_2-O_3-CO_2 photochemical reaction system (Shaheen *et al.,* 2007). The pO_2/pCO_2 ratio affects both the lifespan of $\Delta^{17}O$ anomalies in the troposphere and the magnitude of the stratospheric $\Delta^{17}O$ anomaly (Cao and Bao, 2013). When O_2 with a $\Delta^{17}O$ anomaly is mixed down into the troposphere, it can be consumed by aerobic respiration and replaced by isotopically ''normal'' O_2 produced from photosynthesis (*e.g.,* Luz *et al.,* 1999). It is important to point out that our approach here, as well as that of Cao and Bao (2013), implicitly assumes a constant vertical structure of the atmosphere, and in particular rates of oxygen exchange between the troposphere and stratosphere. This is unlikely to be correct below a certain atmospheric pO_2, as production of O_3 scales nonlinearly with ground-level atmospheric O_2 abundance (Kasting and Donahue, 1980), and this should in turn impact the exchange rates of oxygen between the troposphere and stratosphere. In addition, these models do not fully account for O atom exchange between all atmospheric species (*e.g.,* water vapor). A full evaluation of these issues will require a photochemical model that explicitly tracks O atoms and allows for variable vertical atmospheric structure. Nevertheless, this approach is in keeping with current and previous work, and we consider it a useful starting point from which to move forward.

Because we assume steady state, the model effectively links the overall rate of biospheric O_2 recycling to the oxygen released through primary production within the biosphere. It is important to note that in general biospheric O_2 recycling will likely be less than gross primary productivity (GPP) (with the potential for some deviations induced by photorespiration and the Mehler reaction; see Hodgskiss *et al.,* 2019, for a discussion). As the fraction of photosynthetic O_2 that is exchanged with the environment before being used to recycle gross photosynthate by autotrophic respiration increases, biospheric O_2 recycling approaches GPP. As this fraction drops—for example, most or all of the O_2 used in autotrophic respiration is recycled before leaving the cell, or is produced in an adjacent region of the surface ocean before exchanging with the atmosphere—biospheric O_2 recycling approaches net primary

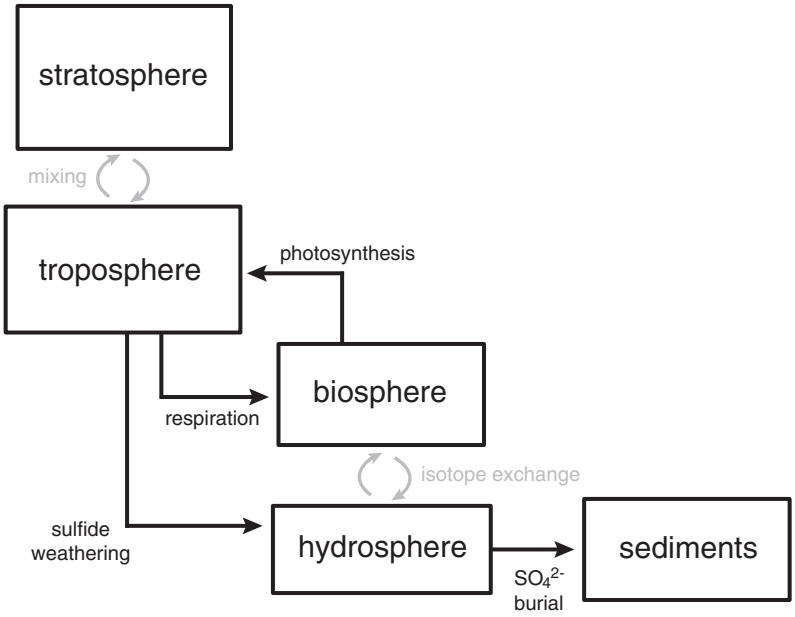

FIG. 2. Schematic overview of the box model used in the first step of our technique for inverting $\Delta^{17}O$ anomalies for atmospheric pO_2. ^{17}O excesses in ozone (O_3) are created in the stratosphere through the Chapman cycle and subsequently transferred to CO_2. Corresponding negative $\Delta^{17}O$ anomalies are transferred to O_2, which can be mixed down into the troposphere where it can be erased through photosynthesis and aerobic respiration (reset to the terrestrial mass fractionation line) or transferred to the rock record via weathering of reduced mineral phases (*e.g.,* pyrite oxidation to form sulfate). The magnitude of $\Delta^{17}O$ transferred to sulfate will be dependent on the atmospheric CO_2/O_2 ratio and the extent of global biospheric O_2 recycling.

productivity. Because the range of pO_2 values consistent with a given $\Delta^{17}O$ value must increase as the rate of biospheric O_2 recycling rises, we consider it conservative for our purposes to use GPP as our metric for biospheric O_2 recycling. We note, however, that the factors regulating this relationship in differing environments and at significantly different O_2 and CO_2 levels are important topics for future work.

Although the amount of primary productivity in the terrestrial realm during the Precambrian is debated, we include a recent lower-end estimate of the oxygen efflux from terrestrial cyanobacterial mats (Planavsky *et al.,* 2018; Zhao *et al.,* 2018). However, it is worth noting that this terrestrial cyanobacterial productivity likely results in an insignificant amount of net organic carbon burial, given the high potential for oxidation during transport of this organic matter to the marine realm. Within this framework, the $\Delta^{17}O$ value of O_2 in the troposphere reflects the mass balance between sourcing of anomalous O_2 from photochemistry in the stratosphere (the magnitude of which varies with the size of the atmospheric CO_2 and O_2 reservoirs) and O_2 recycling within the biosphere (Fig. 2). The tropospheric $\Delta^{17}O$ anomaly can then be transferred to the rock record during pyrite oxidation and subsequent sulfate burial, linking Earth's stratosphere with the rock record.

There are numerous non-unique O_2, CO_2, and GPP combinations that could be consistent with a given sedimentary $\Delta^{17}O$ value (Cao and Bao, 2013; Crockford *et al.,* 2018a). However, not all of these combinations of pO_2, pCO_2, and biospheric recycling will represent mechanistically accessible Earth system states—for example, states that are stable on geologic timescales and satisfy both mass balance within the coupled C-O-S-P cycles and global redox balance. To delineate which combinations of atmospheric O_2, CO_2, and global primary productivity represent plausible alternative Earth states, we rely on previous estimates of atmospheric CO_2 (Sheldon, 2006; Kah and Riding, 2007; Crockford *et al.,* 2018a; Isson and Planavsky, 2018) and combine these with results from a stochastic analysis of the biogeochemical Earth system model CANOPS (Ozaki *et al.,* 2011, 2019) to filter out combinations of pO_2, pCO_2, and GPP that may satisfy $\Delta^{17}O$ mass balance but do not provide redox-balanced Earth system states. The rationale behind this approach is simple—on geologic timescales there are mechanistic links within the Earth system between the globally integrated rate of biospheric primary productivity, organic carbon burial, and atmospheric oxygen levels (Laakso and Schrag, 2014, 2017; Derry, 2015; Ozaki *et al.,* 2019), and these ensure the mass balance and redox balance on geologic timescales.

In practice, our approach occurs in two steps. First, pO_2 and pCO_2 combinations are randomly selected (assuming uniform distributions for both; pO_2 0–100% PAL; pCO_2 2–500 × PAL), and GPP is computed for each pCO_2 and pO_2 combination using our observed minimum $\Delta^{17}O$ value ($\Delta^{17}O = -0.9‰$) as a constraint on our atmosphere-ocean-biosphere model (Fig. 2). This step of the inversion is performed following Crockford *et al.* (2018a) using the parameter ranges listed in Table 1 and results in a wide range of possible atmospheric oxygen levels. To refine these posterior atmospheric pO_2 estimates further, we then filter the data set for combinations of atmospheric pO_2 and GPP that yield mass- and redox-balanced solutions according to a recent stochastic analysis of the CANOPS global biogeochemical model (Figs. 3 and 4; Ozaki *et al.,* 2019). Specifically, we filter the synthetic data set generated from the first resampling analysis for results that fall within the 90% credible interval of mass- and redox-balanced CANOPS results (Fig. 4). This additional filtering step dramatically refines the posterior distribution of atmospheric pO_2 values consistent with the $\Delta^{17}O$ constraint, reducing both the range of pO_2 estimates and their central tendency (Fig. 5). The median pO_2 value yielded by our analysis is 3.4×10^{-3} PAL, with a 90% credible interval of $1.4–8.7 \times 10^{-3}$ PAL (Fig. 5). Although the posterior distribution of pO_2 values still spans over an order of magnitude, this range is considerably more

Table 1. Parameters Used in the Monte Carlo Simulation

Parameter	*Value/Expression*	*Unit*	*Source*
Atmospheric O_2 incorporation into sulfate during pyrite oxidation	8–15%	‰	Balci *et al.,* 2007; Crockford *et al.,* 2018b
Proterozoic terrestrial oxygen flux	1.74	Gt C yr^{-1}	Zhao *et al.,* 2018
Modern GPP (marine)	100	Gt C yr^{-1}	Woodward, 2007
Modern GPP (terrestrial)	120	Gt C yr^{-1}	Woodward, 2007
$\Delta^{17}O_{sulfate}$	-0.9	‰	Crockford *et al.,* 2018b
pCO_2 range explored	0–500	PAL	Kah and Riding, 2007; Sheldon, 2013
pO_2 range explored	10^{-4} to 10^{0}	PAL	
Export production/GPP	0.1		Ozaki *et al.,* 2019

precise than that conventionally invoked for the mid-Proterozoic Earth, which spans well over 2 orders of magnitude (Lyons *et al.,* 2014).

4. Discussion

Given the strong potential to erase $\Delta^{17}O$ anomalies (through surface sulfur cycling) and the stratigraphic rarity of rocks that best preserve atmospheric $\Delta^{17}O$ signals—lacustrine evaporites—we can only reconstruct meaningful maximum pO_2 levels from snapshots of mid-Proterozoic time using this approach. However, we suggest that this snapshot may offer the most robust and precise constraint on surface oxygen levels during mid-Proterozoic time. First, later diagenetic alteration should erase $\Delta^{17}O$ signals for low oxygen, which is in strong contrast to most oxygen proxies for which signals implying low oxygen can potentially be caused by burial diagenesis, alteration, or basin restriction. That is, the $\Delta^{17}O$ system is the only currently available geochemical tracer applicable to the post-Archean rock record that should not be susceptible to ''false positives'' for low O_2. Further, as stressed above, the $\Delta^{17}O$ system is the only known oxygen barometer that records a direct atmospheric signal—with the notable exception of the $\Delta^{33}S$ system, which has transformed our understanding of atmospheric composition during Archean time (4.0–2.5 Ga) (Farquhar *et al.,* 2000; Pavlov and Kasting, 2002; Bekker *et al.,* 2004). The translation of a sulfate $\Delta^{17}O$ value into an atmospheric pO_2 estimate requires a model, and thus the leveraging of several assumptions and consideration of uncertain model parameters. Nevertheless, the use of computationally tractable biogeochemical models allows for formal assessment of uncertainty, and in certain cases should yield significant refinement of pO_2 estimates during Proterozoic time. We consider this approach a useful strategy to build on moving forward, notwithstanding the additional insights likely to emerge from modeling $\Delta^{17}O$ systematics explicitly in 1-D models of atmospheric photochemistry.

Our new atmospheric pO_2 estimate for $\sim$1.4 Ga contrasts with some recent, roughly contemporaneous pO_2 estimates. For example, our estimate is higher than estimates inferred from an early Cr isotope study (<0.1% PAL; Planavsky *et al.,* 2014) but much lower than estimates from several marine redox records (<5% PAL; Zhang *et al.,* 2016a). It is possible that the disagreement among proxies simply reflects time-variable atmospheric oxygen levels, as temporally variable oxygen levels are excepted with a small atmospheric oxygen reservoir. However, we emphasize that the empirical and quantitative approaches utilized in reconstructions of mid-Proterozoic pO_2 that yield estimates outside of 0.1% to 1% PAL range have been strongly critiqued (*e.g.,* Planavsky *et al.,* 2016; Zhang *et al.,* 2016b; Diamond *et al.,* 2018). In any case, our estimate is consistent with a number of other proxy reconstructions. For instance, more recent interpretations of the Proterozoic Cr isotope record, surface oxygen estimates based on cerium oxidation kinetics, and other works revising classical estimates from Proterozoic paleosols are all consistent with a mid-Proterozoic

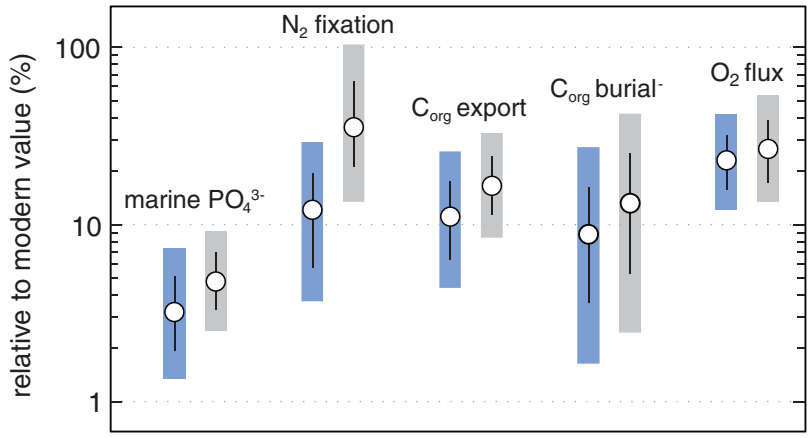

FIG. 3. Example of the steady state environmental parameter space from the CANOPS Monte Carlo simulation with pO_2 ranges of 0.01%–1% PAL (light blue) and 1%–10% PAL pO_2 (light gray). Marine phosphate levels, the extent of N fixation, the marine export flux, organic carbon burial, and the O_2 are all significantly less than those of modern Earth (see Ozaki *et al.,* 2019). Color images are available online.

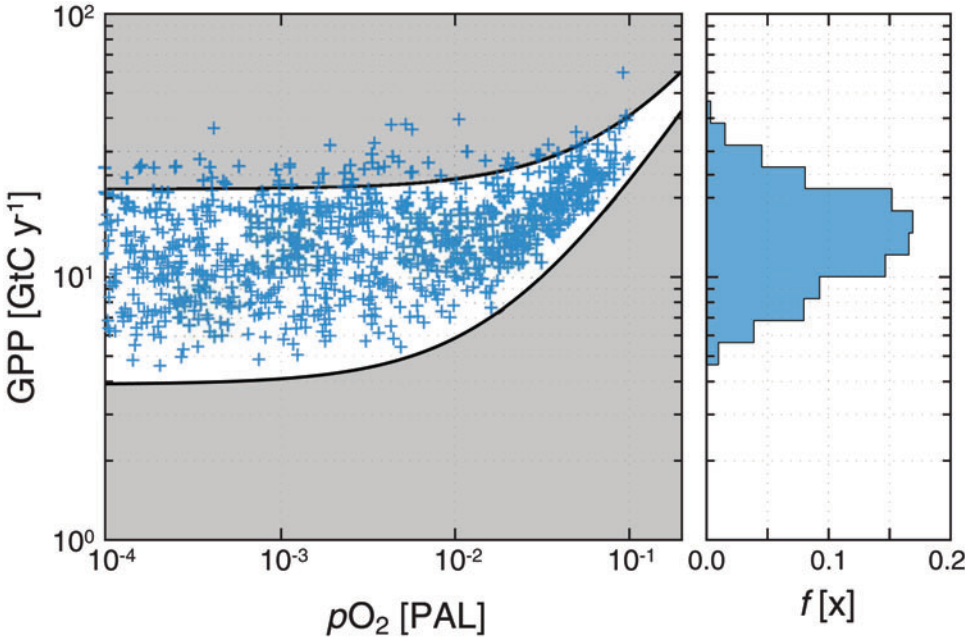

FIG. 4. Mass- and redox-balanced Earth system states from the CANOPS global biogeochemical cycle model. Shown at left are individual CANOPS model runs from the Monte Carlo analysis of Ozaki *et al.* (2019), with the 90% credible interval for combinations of pO_2 (relative to the present atmospheric level, PAL) and gross primary productivity (GPP, in gigatons of carbon per year, GtC y^{-1}) yielding mass- and redox-balanced Earth system states shown by the black lines. The second step of the inversion analysis discussed in the text filters out possible pO_2/pCO_2/GPP combinations that fall within the gray shaded area. Shown at right is a relative frequency distribution of GPP. Color images are available online.

atmospheric pO_2 between 0.1% and 1% PAL (Cole *et al.,* 2016; Gilleaudeau *et al.,* 2016; Liu *et al.,* 2016; Bellefroid *et al.,* 2018).

Robust evidence for low Proterozoic oxygen levels carries important implications for our understanding of long-term ecosystem evolution and the development and maintenance of remotely detectable atmospheric biosignatures. For instance, it has been argued that an Earth system with surface oxygen levels less than ~1% PAL may not be well suited to foster the diversification and expansion of animal-rich ecosystems (Reinhard *et al.,* 2016). Minimum oxygen requirements for many animals are likely less than 1% PAL (Sperling *et al.,* 2015, 2016) but at such low baseline levels of oxygen and productivity would render most marine environments challenging for early metazoan organisms at some stage of the their life history (Reinhard *et al.,* 2016). Second, this work supports the notion that terrestrial planets can maintain "weakly oxygenated" (pO_2 < 1% PAL) states on geologic timescales, rendering certain spectral features of O_2 (and O_3) potentially difficult to discern (see Reinhard *et al.,* 2017, 2019). This provides an impetus to bolster the observational capabilities associated with the most sensitive

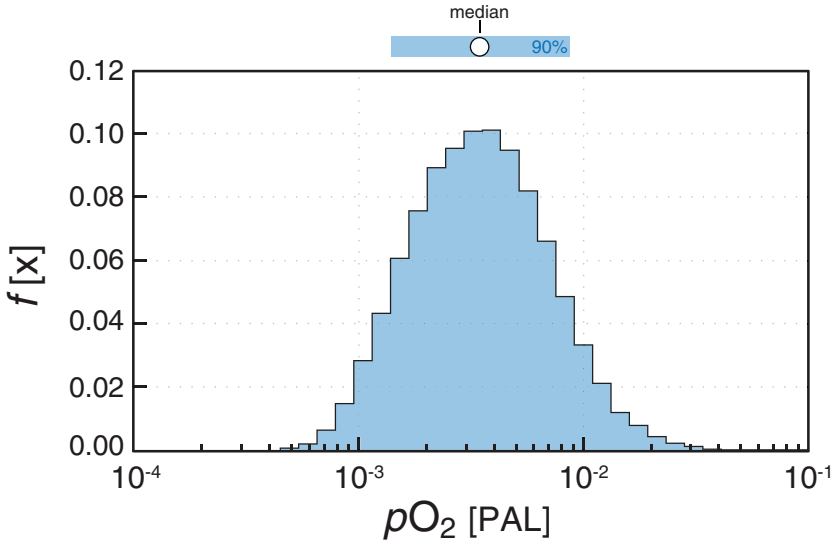

FIG. 5. Atmospheric oxygen estimates consistent with the CANOPS-filtered sulfate $\Delta^{17}O$ values from the inversion analysis. Although there are a wide range of numerically possible O_2, CO_2, primary productivity combinations that are consistent with a single sedimentary $\Delta^{17}O$ value, most of these combinations are not mass- and redox-balanced Earth system states. The stable Earth system states that are consistent with the Sibley $\Delta^{17}O$ data generally have low (<1% PAL) atmospheric oxygen levels. The median value and 90% credible interval for pO_2 are shown above the figure. Color images are available online.

O_2/O_3 spectral features in future direct-imaging exoplanet characterization missions (Schwieterman, 2018).

5. Conclusions

Here we have provided new constraints on atmospheric composition during mid-Proterozoic time by developing a new quantitative technique for interpreting the sedimentary $\Delta^{17}O$ record. Building from previous work that has provided evidence for a less productive mid-Proterozoic biosphere (Crockford *et al.,* 2018a), we translate sulfate $\Delta^{17}O$ values into a range of possible atmospheric oxygen levels by solving for combinations of pO_2, pCO_2, and GPP that are consistent with minimum mid-Proterozoic $\Delta^{17}O$ values for the $\sim$1.4 Ga Sibley Group. Following upon several models that have stressed the mechanistic links between marine nutrient levels, biospheric productivity, and atmospheric oxygen (Laakso and Schrag, 2014, 2017; Derry, 2015; Ozaki *et al.,* 2019), we filter these pO_2/pCO_2/GPP combinations for pO_2 and productivity combinations that yield stable Earth system states in the global biogeochemical model CANOPS. Using this approach, we arrive at an estimate of atmospheric pO_2 at $\sim$1.4 Ga of $3.4^{+5.3}_{-2.0}\times10^{-3}$ times the PAL. Although this approach provides only a snapshot of Earth's evolving atmospheric chemistry, it represents the first quantitative Proterozoic pO_2 estimate from an isotopic signal directly exported by the atmosphere. This bolsters the case that environmental conditions inhibited the rise and diversification of complex multicellular heterotrophs during at least portions of mid-Proterozoic time, and provides impetus for developing observational tools for characterizing weakly oxygenated terrestrial planets beyond the solar system.

Code Availability

The inversion code, all necessary input data, and documentation are hosted on GitHub (http://github.com/reinhard-lab/canops.17O). The version of the code used in this paper is tagged as release v1.0 and has a DOI of 10.5281/zenodo.3715212.

Acknowledgments

This work was funded by the NASA Alternative Earths Astrobiology Institute. The authors thank Bryan Killingsworth and two anonymous reviewers for constructive comments that improved the manuscript and Devon Cole, Dave Johnston, Jim Kasting, and Jingjun Liu for critical discussion.

References

Antler, G., Turchyn, A.V., Rennie, V., Herut, B., and Sivan, O. (2013) Coupled sulfur and oxygen isotope insight into bacterial sulfate reduction in the natural environment. *Geochim Cosmochim Acta* 118:98–117.

Balci, N., Shanks, W.C., Mayer, B., and Mandernack, K.W. (2007) Oxygen and sulfur isotope systematics of sulfate produced by bacterial and abiotic oxidation of pyrite. *Geochim Cosmochim Acta* 71:3796–3811.

Bao, H.M., Lyons, J.R., and Zhou, C.M. (2008) Triple oxygen isotope evidence for elevated CO_2 levels after a Neoproterozoic glaciation. *Nature* 453:504–506.

Bekker, A., Holland, H.D., Wang, P.-L., Rumble, D., III, Stein, H.J., Hannah, J.L., Coetzee, L.L., and Beukes, N.J. (2004) Dating the rise of atmospheric oxygen. *Nature* 427: 117–120.

Bellefroid, E.J., Hood, A.V.S., Hoffman, P.F., Thomas, M.D., Reinhard, C.T., and Planavsky, N.J. (2018) Constraints on Paleoproterozoic atmospheric oxygen levels. *Proc Natl Acad Sci USA* 115:8104–8109.

Canfield, D.E. (1998) A new model for Proterozoic ocean chemistry. *Nature* 396:450–453.

Canfield, D.E. (2005) The early history of atmospheric oxygen: homage to Robert A. Garrels. *Annu Rev Earth Planet Sci* 33: 1–36.

Cao, X.B. and Bao, H.M. (2013) Dynamic model constraints on oxygen-17 depletion in atmospheric O-2 after a snowball Earth. *Proc Natl Acad Sci USA* 110:14546–14550.

Cole, D.B., Reinhard, C.T., Wang, X.L., Gueguen, B., Halverson, G.P., Gibson, T., Hodgskiss, M.S.W., McKenzie, N.R., Lyons, T.W., and Planavsky, N.J. (2016) A shale-hosted Cr isotope record of low atmospheric oxygen during the Proterozoic. *Geology* 44:555–558.

Crockford, P.W., Cowie, B.R., Johnston, D.T., Hoffman, P.F., Sugiyama, I., Pellerin, A., Bui, T.H., Hayles, J., Halverson, G.P., Macdonald, F.A., and Wing, B.A. (2016) Triple oxygen and multiple sulfur isotope constraints on the evolution of the post-Marinoan sulfur cycle. *Earth Planet Sci Lett* 435: 74–83.

Crockford, P.W., Hayles, J.A., Bao, H., Planavsky, N.J., Bekker, A., Fralick, P.W., Halverson, G.P., Bui, T.H., Peng, Y., and Wing, B.A. (2018a) Triple oxygen isotope evidence for limited mid-Proterozoic primary productivity. *Nature* 559: 613–616.

Crockford, P.W., Hodgskiss, M.S.W., Uhlein, G.J., Caxito, F., Hayles, J.A., and Halverson, G.P. (2018b) Linking paleocontinents through triple oxygen isotope anomalies. *Geology* 46:179–182.

Crockford, P.W., Kunzmann, M., Bekker, A., Hayles, J., Bao, H.M., Halverson, G.P., Peng, Y.B., Bui, T.H., Cox, G.M., Gibson, T.M., Worndle, S., Rainbird, R., Lepland, A., Swanson-Hysell, N.L., Master, S., Sreenivas, B., Kuznetsov, A., Krupenik, V., and Wing, B.A. (2019) Claypool continued: extending the isotopic record of sedimentary sulfate. *Chem Geol* 513:200–225.

Derry, L.A. (2015) Causes and consequences of mid-Proterozoic anoxia. *Geophys Res Lett* 42:8538–8546.

Diamond, C.W., Planavsky, N.J., Wang, C., and Lyons, T.W. (2018) What the $\sim$1.4 Ga Xiamaling Formation can and cannot tell us about the mid-Proterozoic ocean. *Geobiology* 16:219–236.

Farquhar, J., Bao, H.M., and Thiemens, M. (2000) Atmospheric influence of Earth's earliest sulfur cycle. *Science* 289:756–758.

Gilleaudeau, G.J., Frei, R., Kaufman, A.J., Kah, L.C., Azmy, K., Bartley, J.K., Chernyavskiy, P., and Knoll, A.H. (2016) Oxygenation of the mid-Proterozoic atmosphere: clues from chromium isotopes in carbonates. *Geochemical Perspectives Letters* 2:178–186.

Hodgskiss, M.S.W., Crockford, P.W., Peng, Y.B., Wing, B.A., and Horner, T.J. (2019) A productivity collapse to end Earth's Great Oxidation. *Proc Natl Acad Sci USA* 116: 17207–17212.

Holland, H.D. (2006) The oxygenation of the atmosphere and oceans. *Philosophical Transactions of the Royal Society B* 361:903–915.

Isson, T.T. and Planavsky, N.J. (2018) Reverse weathering as a long-term stabilizer of marine pH and planetary climate. *Nature* 560:471–473.

Kah, L.C. and Riding, R. (2007) Mesoproterozoic carbon dioxide levels inferred from calcified cyanobacteria. *Geology* 35:799–802.

Killingsworth, B.A., Bao, H.M., and Kohl, I.E. (2018) Assessing pyrite-derived sulfate in the Mississippi River with four years of sulfur and triple-oxygen isotope data. *Environ Sci Technol* 52:6126–6136.

Kohl, I. and Bao, H.M. (2011) Triple-oxygen-isotope determination of molecular oxygen incorporation in sulfate produced during abiotic pyrite oxidation (pH=2–11). *Geochimica Et Cosmochimica Acta* 75:1785–1798.

Kump, L.R. (2008) The rise of atmospheric oxygen. *Nature* 451:277–278.

Laakso, T.A. and Schrag, D.P. (2014) Regulation of atmospheric oxygen during the Proterozoic. *Earth Planet Sci Lett* 388:81–91.

Laakso, T.A. and Schrag, D.P. (2017) A theory of atmospheric oxygen. *Geobiology* 15:366–384.

Liu, X.M., Kah, L.C., Knoll, A.H., Cui, H., Kaufman, A.J., Shahar, A., and Hazen, R.M. (2016) Tracing Earth's O-2 evolution using Zn/Fe ratios in marine carbonates. *Geochem Perspect Lett* 2:24–34.

Luz, B., Barkan, E., Bender, M.L., Thiemens, M.H., and Boering, K.A. (1999) Triple-isotope composition of atmospheric oxygen as a tracer of biosphere productivity. *Nature* 400:547–550.

Lyons, T.W., Reinhard, C.T., and Planavsky, N.J. (2014) The rise of oxygen in Earth's early ocean and atmosphere. *Nature* 506:307–315.

Mitchell, R.L. and Sheldon, N.D. (2009) Weathering and paleosol formation in the 1.1 Ga Keweenawan Rift. *Precambrian Res* 168:271–283.

Mitchell, R.L. and Sheldon, N.D. (2010) The similar to 1100 Ma Sturgeon Falls paleosol revisited: implications for Mesoproterozoic weathering environments and atmospheric CO_2 levels. *Precambrian Res* 183:738–748.

Mitchell, R.L. and Sheldon, N.D. (2016) Sedimentary provenance and weathering processes in the 1.1 Ga Midcontinental Rift of the Keweenaw Peninsula, Michigan, USA. *Precambrian Res* 275:225–240.

Ozaki, K., Tajima, S., and Tajika, E. (2011) Conditions required for oceanic anoxia/euxinia: constraints from a one-dimensional ocean biogeochemical cycle model. *Earth Planet Sci Lett* 304:270–279.

Ozaki, K., Reinhard, C.T., and Tajika, E. (2019) A sluggish mid-Proterozoic biosphere and its effect on Earth's redox balance. *Geobiology* 17:3–11.

Pavlov, A.A. and Kasting, J.F. (2002) Mass-independent fractionation of sulfur isotopes in Archean sediments: strong evidence for an anoxic Archean atmosphere. *Astrobiology* 2:27–41.

Peng, Y.B., Bao, H.M., Pratt, L.M., Kaufman, A.J., Jiang, G.Q., Boyd, D., Wang, Q.X., Zhou, C.M., Yuan, X.L., Xiao, S.H., and Loyd, S. (2014) Widespread contamination of carbonate-associated sulfate by present-day secondary atmospheric sulfate: evidence from triple oxygen isotopes. *Geology* 42: 815–818.

Petrash, D.A., Gingras, M.K., Lalonde, S.V., Orange, F., Pecoits, E., and Konhauser, K.O. (2012) Dynamic controls on accretion and lithification of modern gypsum-dominated thrombolites, Los Rogues, Venezuela. *Sedimentary Geology* 245:29–47.

Pinto, J.P. and Holland, H.D. (1988) Paleosols and the evolution of the atmosphere; part II. In *Paleosols and Weathering through Geologic Time: Principles and Applications,* edited by J. Reinhardt and W.R. Sigleo, Geological Society of America, Denver, CO, pp 21–34.

Planavsky, N.J., Reinhard, C.T., Wang, X.L., Thomson, D., McGoldrick, P., Rainbird, R.H., Johnson, T., Fischer, W.W., and Lyons, T.W. (2014) Low Mid-Proterozoic atmospheric oxygen levels and the delayed rise of animals. *Science* 346: 635–638.

Planavsky, N.J., Cole, D.B., Reinhard, C.T., Diamond, C., Love, G.D., Luo, G.M., Zhang, S., Konhauser, K.O., and Lyons, T.W. (2016) No evidence for high atmospheric oxygen levels 1,400 million years ago. *Proc Natl Acad Sci USA* 113:E2550–E2551.

Planavsky, N.J., Cole, D.B., Isson, T.T., Reinhard, C.T., Crockford, P.W., Sheldon, N.D., and Lyons, T.W. (2018) A case for low atmospheric oxygen levels during Earth's middle history. *Emerg Top Life Sci* 2:149–159.

Poulton, S.W., Fralick, P.W., and Canfield, D.E. (2010) Spatial variability in oceanic redox structure 1.8 billion years ago. *Nat Geosci* 3:486–490.

Reinhard, C.T., Planavsky, N.J., Olson, S.L., Lyons, T.W., and Erwin, D.H. (2016) Earth's oxygen cycle and the evolution of animal life. *Proc Natl Acad Sci USA* 113:8933–8938.

Reinhard, C.T., Olson, S.L., Schwieterman, E.W., and Lyons, T.W. (2017) False negatives for remote life detection on ocean-bearing planets: lessons from the early Earth. *Astrobiology* 17:287–297.

Reinhard, C.T., Schwieterman, E.W., Olson, S.L., Planavsky, N.J., Arney, G.N., Ozaki, K., Som, S., Robinson, T.D., Domagal-Goldman, S.D., Lisman, D., Mennesson, B., Meadows, V.S., and Lyons, T.W. (2019) The remote detectability of Earth's biosphere through time and the importance of UV capability for characterizing habitable exoplanets. [White paper submitted in response to the solicitation of feedback for the Decadal Survey on Astronomy and Astrophysics (Astro 2020) by the National Academy of Sciences] arXiv: 1903.05611

Schwieterman, E., Reinhard, C.T., Olson, S., and Lyons, T.W. (2018) The Importance of UV capabilities for identifying inhabited exoplanets with next generation space telescopes. [White paper submitted in response to the NAS Astrobiology Science Strategy for the Search for Life in the Universe] arXiv:1801.02744

Shaheen, R., Janssen, C., and Rockmann, T. (2007) Investigations of the photochemical isotope equilibrium between O_2, CO_2 and O_3. *Atmos Chem Phys* 7:495–509.

Sheldon, N.D. (2006) Precambrian paleosols and atmospheric CO_2 levels. *Precambrian Res* 147:148–155.

Sheldon, N.D. (2013) Causes and consequences of low atmospheric pCO_2 in the Late Mesoproterozoic. *Chem Geol* 362: 224–231.

Sperling, E.A., Knoll, A.H., and Girguis, P.R. (2015) The ecological physiology of Earth's second oxygen revolution. *Annu Rev Ecol Evol Syst* 46:215–235.

Sperling, E.A., Carbone, C., Strauss, J.V., Johnston, D.T., Narbonne, G.M., and Macdonald, F.A. (2016) Oxygen, facies, and secular controls on the appearance of Cryogenian and Ediacaran body and trace fossils in the Mackenzie Mountains of northwestern Canada. *Geol Soc Am Bull* 128:558–575.

Thiemens, M.H. (2006) History and applications of mass-independent isotope effects. *Annu Rev Earth Planet Sci* 34: 217–262.

Thiemens, M.H. and Heidenreich, J.E. (1983) The mass-independent fractionation of oxygen—a novel isotope effect and its possible cosmochemical implications. *Science* 219: 1073–1075.

Urey, H.C. (1947) The thermodynamic properties of isotopic substances. *Journal of the Chemical Society* 0:562–581.

Woodward, F.I. (2007) Global primary production. *Current Biology* 17:R269–R273.

Yakushev, E.V. and Neretin, L.N. (1997) One-dimensional modeling of nitrogen and sulfur cycles in the aphotic zones of the Black and Arabian Seas. *Global Biogeochem Cycles* 11:401–414.

Zbinden, E.A., Holland, H.D., Feakes, C.R., and Dobos, S.K. (1988) The Sturgeon Falls paleosol and the composition of the atmosphere 1.1 Ga Bp. *Precambrian Res* 42:141–163.

Zhang, S., Wang, X., Wang, H., Bjerrum, C., Hammarlund, E.U., Costa, M.M., Connelly, J.N., Zhang, B., Sua, J., and Canfield, D.E. (2016a) Sufficient oxygen for animal respiration 1,400 million years ago. *Proc Natl Acad Sci USA* 113:1731–1736.

Zhang, S.C., Wang, X.M., Wang, H.J., Bjerrum, C.J., Hammarlund, E.U., Dahl, T.W., and Canfield, D.E. (2016b) Reply to Planavsky *et al.*: strong evidence for high atmospheric oxygen levels 1,400 million years ago. *Proc Natl Acad Sci USA* 113:E2552–E2553.

Zhao, M.Y., Reinhard, C.T., and Planavsky, N. (2018) Terrestrial methane fluxes and Proterozoic climate. *Geology* 46: 139–142.

Address correspondence to:
Noah J. Planavsky
Department of Geology and Geophysics
Yale University
210 Whitney Ave.
New Haven, CT 06511

E-mail: noah.planavsky@yale.edu

Submitted 3 March 2019
Accepted 13 January 2020

Abbreviations Used

GPP = gross primary productivity
NMD = non-mass-dependent
PAL = present atmospheric level